Cellular and Molecular Life Sciences (2018) 75:2045–2058
https://doi.org/10.1007/s00018-017-2720-9

ORIGINAL ARTICLE

Blockage of the NLRP3 inflammasome by MCC950 improves anti-tumor immune responses in head and neck squamous cell carcinoma

Lei Chen[1] · Cong-Fa Huang[1] · Yi-Cun Li[1] · Wei-Wei Deng[1] · Liang Mao[1] · Lei Wu[1] · Wen-Feng Zhang[1,2] · Lu Zhang[1,3] · Zhi-Jun Sun[1,2]

Received: 3 June 2017 / Revised: 12 November 2017 / Accepted: 22 November 2017 / Published online: 28 November 2017

Abstract

The NLRP3 inflammasome is a critical innate immune pathway responsible for producing active interleukin (IL)-1β, which is associated with tumor development and immunity. However, the mechanisms regulating the inflammatory microenvironment, tumorigenesis and tumor immunity are unclear. Herein, we show that the NLRP3 inflammasome was over-expressed in human HNSCC tissues and that the IL-1β concentration was increased in the peripheral blood of HNSCC patients. Additionally, elevated NLRP3 inflammasome levels were detected in tumor tissues of *Tgfbr1/Pten* 2cKO HNSCC mice, and elevated IL-1β levels were detected in the peripheral blood serum, spleen, draining lymph nodes and tumor tissues. Blocking NLRP3 inflammasome activation using MCC950 remarkably reduced IL-1β production in an HNSCC mouse model and reduced the numbers of myeloid-derived suppressor cells (MDSCs), regulatory T cells (Tregs) and tumor-associated macrophages (TAMs). Moreover, inhibiting NLRP3 inflammasome activation increased the numbers of $CD4^+$ and $CD8^+$ T cells in HNSCC mice. Notably, the numbers of exhausted PD-1^+ and $Tim3^+$ T cells were significantly reduced. A human HNSCC tissue microarray showed that NLRP3 inflammasome expression was correlated with the expression of CD8 and CD4, the Treg marker Foxp3, the MDSC markers CD11b and CD33, and the TAM markers CD68 and CD163, PD-1 and Tim3. Overall, our results demonstrate that the NLRP3 inflammasome/IL-1β pathway promotes tumorigenesis in HNSCC and inactivation of this pathway delays tumor growth, accompanied by decreased immunosuppressive cell accumulation and an increased number of effector T cells. Thus, inhibition of the tumor microenvironment through the NLRP3 inflammasome/IL-1β pathway may provide a novel approach for HNSCC therapy.

Keywords NLRP3 inflammasome · IL-1β · Immunosuppressive cells · PD-1 · Tim3 · HNSCC

Abbreviations

NLRP3	Nod-like receptor protein 3
HNSCC	Head and neck squamous cell carcinoma
Dys	Dysplasia
IL-1β	Interleukin (IL)-1β
TILs	Tumor-infiltrating lymphocytes
Tregs	Regulatory T cells
TCGA	The Cancer Genome Atlas
MDSCs	Myeloid-derived suppressor cells
TAMs	Tumor-associated macrophages
PD-1	Programmed death-1

Electronic supplementary material The online version of this article (https://doi.org/10.1007/s00018-017-2720-9) contains supplementary material, which is available to authorized users.

Lei Chen and Cong-Fa Huang contributed equally to this study.

✉ Zhi-Jun Sun
sunzj@whu.edu.cn

Lu Zhang
luzhang2012@whu.edu.cn

[1] The State Key Laboratory Breeding Base of Basic Science of Stomatology (Hubei-MOST) and Key Laboratory of Oral Biomedicine Ministry of Education, School and Hospital of Stomatology, Wuhan University, Wuhan, China

[2] Department of Oral Maxillofacial-Head Neck Oncology, School and Hospital of Stomatology, Wuhan University, Wuhan, China

[3] Department of Endodontics, School and Hospital of Stomatology, Wuhan University, Wuhan, China

Tim3 T cell immunoglobulin mucin-3
ELISA Enzyme-linked immunosorbent assay

Introduction

While inflammation is critical for the host innate immune system to combat pathogens, cumulative studies have shown that inflammation plays an important role in tumor initiation and development [1, 2]. However, the mechanism of the innate immune-derived inflammatory microenvironment in tumor progression is still unclear. The inflammasome is a critical innate immune pathway for the production of active IL-1β, a key inflammatory cytokine [3], which acts as a double-edged sword, since it not only participates in host defense but is also related to autoimmune disease and cancer [4]. As the most extensively studied inflammasome, the NLRP3 (nod-like receptor protein 3) inflammasome is composed of the NLRP3 scaffold, the adaptor apoptosis-associated speck-like protein containing a caspase recruitment domain (ASC), and caspase-1, which is responsible for the cleavage of the pro-IL-1β and pro-IL-18 proteins into their active forms. The abnormal secretion of IL-1β has been implicated in a variety of autoimmune diseases and tumors [5] and is correlated with worse survival for patients with certain cancers [6, 7]. Currently, little is known about the roles of the NLRP3 inflammasome and IL-1β pathway in the inflammatory microenvironment and tumor immunity.

With approximately 48,100 new cases per year in China and a mortality rate as high as 50% in 2015 [8], head and neck squamous cell carcinoma (HNSCC) ranks sixth among the most common cancers in the world [9]. Despite our improved understanding of cancer, the 5-year survival rate (50%) of HNSCC patients has remained relatively unchanged in the past three decades [10]. Extensive studies have shown that HNSCC is an immunosuppressive malignancy [11] that is characterized by impaired antigen-presenting capacity [12], impaired NK cell function [13], a lower number of lymphocytes and the presence of immunosuppressive cells [14, 15]. Recently, studies have shown that the inflammasome and IL-1β pathway could regulate myeloid cell recruitment and promote tumor growth and metastasis in breast cancer [16]. However, the mechanism of how inflammation affects tumor immunity in HNSCC is unclear.

The accumulation of immunosuppressive cells, including myeloid-derived suppressor cells (MDSCs), regulatory T cells (Tregs), and tumor-associated macrophages (TAMs), which can impair the T cell response and result in an immunosuppressive state in tumor patients, means that tumorigenesis may occur more readily [17]. In addition, chronic inflammation could induce immunosuppression in cancer patients, and in this process, suppressor cell-like MDSCs, Tregs and TAMs are induced, but immune cells, such as T cells and NK cells, are suppressed [18]. The knockout of NLRP3 in mice can effectively reduce the population of MDSCs [19] and TAMs [16]. However, the mechanism of how inflammation affects tumor immunity is unclear. Accumulating evidence has demonstrated that Tregs, MDSCs and TAMs are related to the immunosuppressive state in HNSCC [20, 21]. Immune checkpoint blockade therapies have demonstrated that an endogenous immune response can cause regression of human tumors [22]. Dysregulation of programmed death-1 (PD-1) and T cell immunoglobulin mucin-3 (Tim3) can also cause immune resistance in HNSCC [21, 23]. Inflammasome-mediated IL-1β can induce the recruitment of TAMs and MDSCs, which promotes breast cancer development [16]. Although the NLRP3 inflammasome plays an important role in the inflammatory microenvironment, the immune response against infections and tumor development, the role of NLRP3 inflammasome/IL-1β signaling in the inflammatory microenvironment and tumor immunity remains poorly characterized in HNSCC. In this study, we investigated NLRP3 inflammasome/IL-1β expression in both mouse and human HNSCC, and analyzed the relationship between the NLRP3 inflammasome, immunosuppressive cell markers and the immune checkpoint proteins, PD-1 and Tim3, in HNSCC patients. Moreover, we explored the variation of HNSCC immunity in mice after NLRP3 inactivation.

Materials and methods

Reagents

NLRP3 inhibitor MCC950 (PZ0280) was purchased from Sigma-Aldrich (St. Louis, MO, USA), and human and mouse IL-1β ELISA kits were purchased from Dakewe BioTech (Beijing, China). Antibodies for immunohistochemistry, immunofluorescence and western blotting: caspase-1, IL-1β, Foxp3, CD8, CD4, PD-1,Tim3 and SIRPα were from Cell Signaling Technology (Boston, MA, USA); IL-18, CD11b, and CD47 were from Abcam (Cambridge, UK); CD8, CD68 and CD33 were from Zymed (San Diego, CA, USA); ASC and CXCL1 were from GeneTex Inc. (Irvine, CA, USA); CD4 and Ly6G were from Service Bio (Wuhan, China); CD11b and CCL2 were from Novus Biologicals (Littleton, CO, USA); CD163 was from CWBiotech (Beijing, China); NLRP3 was from Sigma-Aldrich (St. Louis, MO, USA); and CK14 was from PROGEN (Heidelberg, Germany). All antibodies for flow cytometry were purchased from eBioscience (San Diego, CA, USA): PE-conjugated LY6G, Foxp3, PD-1, Tim3 and F4/80, PE-Cy7-conjugated LY6C, FITC-conjugated CD4 and CD11b, PE-Cy5-conjugated CD8, and APC-conjugated CD25.

Mice

The mice used in this experiment were inducible and tissue-specific HNSCC mouse models [24]; 4–8-week-old *Tgfbr1/Pten* 2cKO mice (*K14-Cre*^{tam}; *Tgfbr1*$^{flox/flox}$; *Pten*$^{flox/flox}$) received five consecutive days of tamoxifen gavage to conditionally delete *Tgfbr1* and *Pten* in mice head and neck epithelia, which may cause the activation of PI3K/Akt pathway and increased secretion of TGF-β; finally, squamous cell carcinoma was formed in the head and neck of these mice with complete penetrance and immunocompetence [24]. *Tgfbr1*$^{flox/flox}$/*Pten*$^{flox/flox}$ mice from the same litter were used as the control. All the mice were maintained in FVBN/CD1/129/C57 mixed background. Animal studies were approved and supervised by the Animal Care and Use Committee of Wuhan University.

MCC950 in vivo treatment

Tgfbr1/Pten 2cKO mice ($n = 18$) were randomly divided into three groups after tamoxifen was induced. MCC950 was administered i.p. (10 mg/kg or 15 mg/kg) every day for the first 3 days and every second day for the next 20 days. Starting treatment was at day 14, after gavage and PBS was intraperitoneally injected into mice as the negative control. The tumor volume was calculated every day by a micrometer caliper. Mice were killed at day 49 after gavage, and the spleen, blood, draining lymph nodes, and tumor were separated and immediately preserved.

Human peripheral blood

Human blood collected from healthy donors and HNSCC donors was collected from the Hospital of Stomatology at Wuhan University. Research Blood Components tested each donor's blood for standard blood-borne pathogens prior to the initial donation and at the time of each subsequent donation. Only blood samples negative for HIV, HTLV, HCV and HBV were used. Written informed consent was obtained from all participants.

Tissue microarrays

The human HNSCC tissue microarrays (TMA) used in this study contained 64 primary HNSCC, 38 normal oral mucosae and 12 oral epithelial dysplasia (Dys); there are still some other categories that were not included in this experiment. These specimens were collected from January 2008 to August 2014 in the Department of Oral and Maxillofacial Surgery, School and Hospital of Stomatology, Wuhan University. The clinical stages of HNSCC were classified according to International Union Against Cancer (UICC 2002) guidelines, and histological grading was determined according to the scheme of the World Health Organization. All studies obtained informed consent from patients at the beginning of the trial and were approved by the Medical Ethics Committee of the Hospital of Stomatology, Wuhan University.

ELISA assays

Fresh human or mice blood and tissue homogenates (1 g tissue/mL PBS) were centrifuged for 20 min at 3000 rpm for the supernatants. IL-1β concentration in the supernatants of human and mice samples was determined by IL-1β Enzyme-linked immunosorbent Assay Kit (Dakewe BioTech, Beijing, China) per the manufacturer's instructions.

Flow cytometry

For flow cytometry, single-cell suspensions of spleen, blood, lymph nodes and tumor were resuspended in PBS buffer (2% FBS) and non-specific Fc was blocking for 10 min at 4 °C, and then cells were stained with the abovementioned fluorochrome-conjugated monoclonal antibodies. For the staining of non-cell surface marker Foxp3, the cell membrane was penetrated according to the manufacturer's instructions (eBioscience, San Diego, CA, USA) before antibody incubation. Samples were acquired on a NovoCyte Flow Cytometer (ACEA NovoCyte™, San Diego, CA, USA), and data were analyzed by its corresponding software, NovoExpress. Isotype-matched IgG antibody was used as a control in the experiment.

Immunohistochemistry

For the immunohistochemistry, 4-μm sections of paraffin-embedded tissue were heated in sodium citrate solution medium until boiling was initiated, which lasted 5 min for antigen unmasking. Sections were incubated in 3% hydrogen peroxide for 20 min at 37 °C to quench endogenous peroxidase activity. Then, 10% normal goat serum (ZSGB-BIO, Beijing, China) was used to block non-specific binding for 20 min at 37 °C and incubated overnight at 4 °C with specific primary antibodies at the appropriate dilutions. After 1 h, sections were incubated with corresponding secondary biotinylated immunoglobulin G antibody solution and an avidin–biotin–peroxidase reagent at room temperature and were stained with the DAB kit (Mxb Biotechnologies, Fuzhou, China) then lightly counterstained with Mayer's hematoxylin (Invitrogen, Carlsbad, CA, USA). Immunohistochemistry of human HNSCC tissue microarrays was performed in the same way. Each antibody was provided by the PBS negative control group and corresponding positive control group.

Immunofluorescence

For the immunofluorescence, all the steps before adding fluorochrome conjugated secondary antibodies were the same as those for immunohistochemistry. Sections were incubated with corresponding fluorescent antibodies (DyLight 488 anti-rabbit and anti-mouse, DyLight 594 anti-rabbit and anti-mouse; Thermo Fisher Scientific, Waltham, MA, USA) for 1 h in the dark at 37 °C and then mounted by anti-fluorescence quenching medium with DPAI (Vector, Burlingame, CA, USA). The slides were observed by a fluorescence microscope (CLSM-310, ZEISS fluorescence microscope, Germany) or confocal laser scanning microscope (FV300, Olympus Life Science, Tokyo, Japan).

Western blot

Tumor tissues were harvested after mice sacrifices and lysed by RIPA reagent (Pierce, Rockford, IL, USA), which was pre-added with protease and phosphatase inhibitors. Then, the protein lysates were generated after ultrasonic processing and centrifugation. After denaturing in a loading buffer (Service Bio, Wuhan, China), proteins from lysates were resolved in 8–12% SDS–polyacrylamide gel and transferred to polyvinylidene fluoride (PVDF) membrane (Merck Millipore, Billerica, MA, USA). Membranes were blocked with 5% skim milk for 1 h at room temperature, and incubated overnight at 4 °C with specific primary antibodies at the appropriate dilutions. After 1 h, membranes were incubated with secondary HRP-conjugated antibody at room temperature; the blots were detected with an ECL kit (Advansta Inc., Menlo Park, CA, USA).

Scoring system and hierarchical clustering

All slides were scanned by an Aperio ScanScope CS scanner (Aperio, San Diego, CA, USA) with background subtraction. The histoscore quantification of each sample was analyzed by the Aperio Quantification System (Version 9.1) [24]. For hierarchical clustering, the histoscore of each biomarker was converted into scaled values centered on zero (–3–0–3) in Microsoft Excel, and then hierarchical analysis was performed by the Cluster 3.0, with average linkage based on Pearson's correlation coefficient [25]. Java TreeView 1.1.6 was used to visualize the results [26]. Finally, the clustered data and tissue samples were arranged on the horizontal and vertical axes, respectively. Biomarkers with a close relationship were located next to each other.

Statistical analysis

GraphPad Prism 7.0 (GraphPad Software, Inc., La Jolla, CA, USA) was applied in statistical analysis. Unpaired or paired *t* tests were adopted for data between two groups. One-way ANOVA was used for data between multiple groups. Two-tailed Pearson's statistics were applied in correlation analysis. Data were presented as mean ± SEM, and significance was determined as $p < 0.05$.

Results

NLRP3 inflammasome expression was elevated in human HNSCC and in a mouse model of HNSCC

To determine the expression of the NLRP3 inflammasome and IL-1β in HNSCC, we performed immunohistochemical staining on the following human HNSCC tissue samples: 38 samples of normal oral mucosa, 12 cases of dysplasia (Dys) and 64 cases of human HNSCC. We found increased expression of the NLRP3 inflammasome components NLRP3, ASC, caspase-1 and IL-18 in human HNSCC compared with the dysplastic and mucosal samples (Fig. 1a). The NLRP3 inflammasome served as the main activating platform for IL-1β; to investigate whether a similar variation of IL-1β was expressed in human HNSCC, based on the analysis of the online Oncomine® databases we found that the *IL-1B* mRNA level was higher in human HNSCC tissue than in normal mucosa in Peng, Ye and Ginos Head–Neck dataset [27–29] (Fig. 1b and Fig. S1a). This result was also validated in the TCGA database (Fig. 1c). Moreover, our ELISA results confirmed that the concentration of IL-1β was significantly elevated in the peripheral blood of HNSCC patients compared with healthy donors (HD, $n = 10$; HNSCC, $n = 10$; Fig. 1d). In addition, a spontaneous de novo HNSCC mouse model was adopted for in vivo experiments. Similarly, NLRP3, ASC, caspase-1 and IL-18 were found to be overexpressed in *Tgfbr1*/*Pten* 2cKO HNSCC mice tumor tissue (Fig. 1e), and according to an ELISA, the expression of IL-1β was heightened in the peripheral blood, spleen, draining lymph nodes (DLN) and tumor homogenates of spontaneous HNSCC mice in comparison with wild-type mice (Fig. 1f).

The inhibition of NLRP3 inflammasome activity delayed tumorigenesis in a mouse model of HNSCC

To evaluate the roles of the NLRP3 inflammasome and IL-1β in tumor growth, we took advantage of our spontaneous de novo HNSCC mouse model, which exhibits constant activation of NLRP3 inflammasome/IL-1β signaling. We examined the efficacy of chemopreventive inhibition of NLRP3 inflammasome by the specific small molecule inhibitor MCC950. Tumor growth was assessed every day after tamoxifen gavage. Indeed, the results showed that MCC950 treatment at a dose of 10 mg/kg significantly delayed the

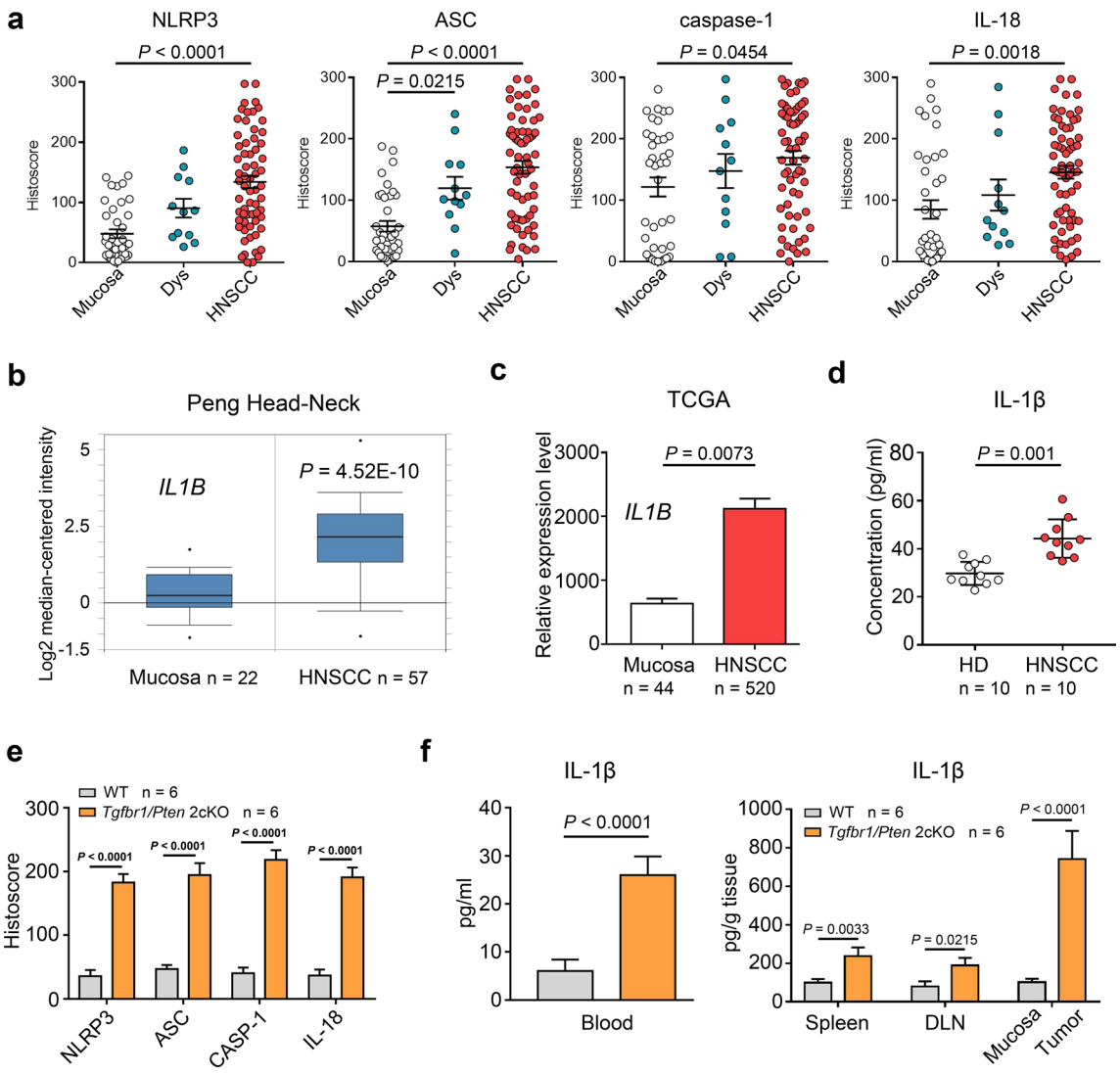

Fig. 1 The NLRP3 inflammasome was overexpressed in both human and mice HNSCC. **a** Immunohistochemical histoscore of NLRP3, caspase-1, ASC, and IL-18 in the oral mucosa ($n = 38$), dysplasia (Dys, $n = 12$), and head and neck squamous cell carcinoma (HNSCC, $n = 64$), one-way ANOVA test. **b** *IL1B* mRNA expression levels from Peng Head–Neck dataset (as log2 median-centered ratio) for head–neck cancer versus its normal counterpart (t test, $p = 4.52\text{E}{-10}$). **c** *IL1B* mRNA expression level analysis in 44 normal mucosae and 520 HNSCC tissue from TCGA dataset (t test, $p = 0.0073$). **d** The concentration of IL-1β in human peripheral blood was measured by ELISA (10 HD (healthy donor) and 10 HNSCC, t test, $p = 0.001$). **e** Quantitative histoscores in NLRP3, caspase-1, ASC and IL-18 were significantly higher in *Tgfbr1/Pten* 2cKO mice ($n = 6$) than in WT mice ($n = 6$), t test. **f** IL-1β was up-regulated in various tissues of *Tgfbr1/Pten* 2cKO tumor-bearing mice ($n = 6$) compared with wild-type mice ($n = 6$), t test. All data are presented as mean ± SEM

progression of tumor growth and that MCC950 treatment at a dose of 15 mg/kg induced a better effect ($*p < 0.05$, $**p < 0.01$; Fig. 2a). The ELISA results showed that the level of IL-1β was significantly reduced in peripheral blood serum, spleen, draining lymph nodes and tumor tissues after MCC950 treatment (15 mg/kg) (Fig. 2b). In addition, the *Tgfbr1/Pten* 2cKO tumor-bearing mice were in a state of immune dysregulation, in which the mice exhibited the characteristics of lymphadenopathy and splenomegaly [21, 30, 31]. However, we observed that the sizes of the lymph nodes and spleen were decreased after MCC950 treatment (Fig. 2c, d), which might indicate that the immunosuppressive state of tumor-bearing mice may have been partially alleviated.

Inactivation of the NLRP3 inflammasome reduced the number of regulatory T cells in a mouse model of HNSCC

The presence of regulatory T cells (Tregs) is one cause of an immunosuppressive state in tumor-bearing individuals, and these cells may be distinguished by the specific molecular markers CD4, CD25 and Foxp3 [32].

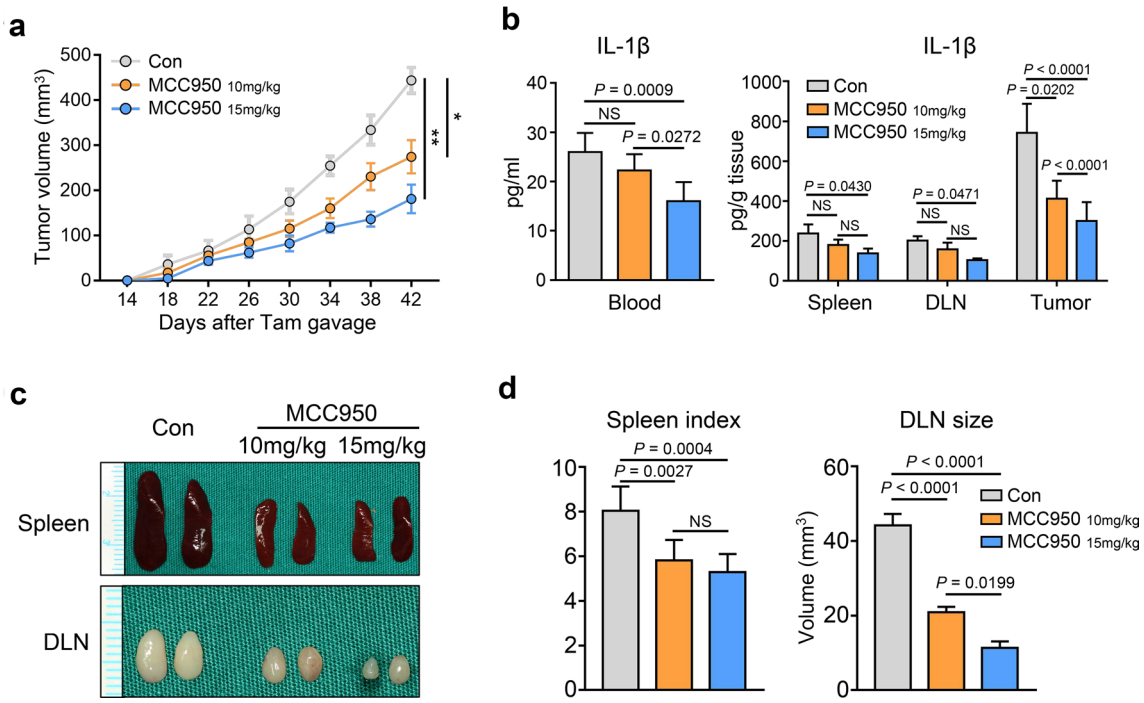

Fig. 2 MCC950 treatment reduced the production of IL-1β and retarded tumorigenesis in a HNSCC mouse model. **a** Tumor volume was monitored after tamoxifen gavage in *Tgfbr1*/*Pten* 2cKO mice. Six mice in each group (*$p < 0.05$, **$p < 0.01$). **b** IL-1β levels in 2cKO tumor-bearing mice blood, spleen, DLN, and tumor were dropped after MCC950 treatment, one-way ANOVA test. **c** Representative photos of spleen and draining lymph nodes in three groups show that MCC950 could reduce the spleen and lymph node volume. **d** Spleen index shows the significant differences (left panel, one-way ANOVA test), and the sizes of lymph nodes were measured (right panel, one-way ANOVA test). All data are presented as mean ± SEM

Moreover, our previous data demonstrated that the proportion of Tregs was notably increased in *Tgfbr1*/*Pten* 2cKO HNSCC mice [21]. In the present study, using flow cytometry, we found that the number of Tregs was decreased in the group treated with MCC950 (10 and 15 mg/kg) (Fig. 3a). Nevertheless, the population of $CD4^+Foxp3^+CD25^+$ cells in the spleen was significantly reduced in the 15 mg/kg MCC950 treatment group compared with the 10 mg/kg MCC950 treatment group and the control group (Fig. 3b). In blood samples, the number of $CD4^+Foxp3^+CD25^+$ cells was decreased in both the 10 and the 15 mg/kg MCC950 treatment groups (Fig. 3b). However, we did not observe meaningful changes in the proportion of Tregs after MCC950 treatment in the DLN samples (Fig. 3b). Furthermore, the immunochemistry results showed that Foxp3-positive cells in tumor tissues of mice in the MCC950 treatment group (10 and 15 mg/kg) were obviously fewer in number than in the control group (Fig. 3c, d). These results demonstrated that a subset of Tregs in the tumor microenvironment was decreased after MCC950 treatment in *Tgfbr1*/*Pten* 2cKO HNSCC mice.

Inactivation of the NLRP3 inflammasome diminished MDSCs and TAMs in a mouse model of HNSCC

Recently, studies have shown that MDSCs and M2 macrophages can function as negative regulators of the antitumor immune response in HNSCC [20, 23] and that both of these cell types appear in large numbers in *Tgfbr1*/*Pten* 2cKO HNSCC mice [21]. MDSCs can be further divided into $CD11b^+LY6G^-LY6C^{high}$ monocytic and $CD11b^+LY6G^+LY6C^{low}$ granulocytic MDSCs; these two subsets have different functions in cancer, and almost all tumor types have demonstrated a preferential expansion of the granulocytic subset [33]. Not surprisingly, the flow cytometry results showed that the proportion of $LY6C^{high}$ monocytic MDSCs did not noticeably change and accounted for only a small proportion of MDSCs (Fig. 4a). However, the proportion of $LY6G^+$ granulocytic MDSCs was significantly decreased after NLRP3 inflammasome blockade in spleen and tumor tissues (Fig. 4b, c), and we observed that the proportion of granulocytic MDSCs was higher than that of monocytic MDSCs

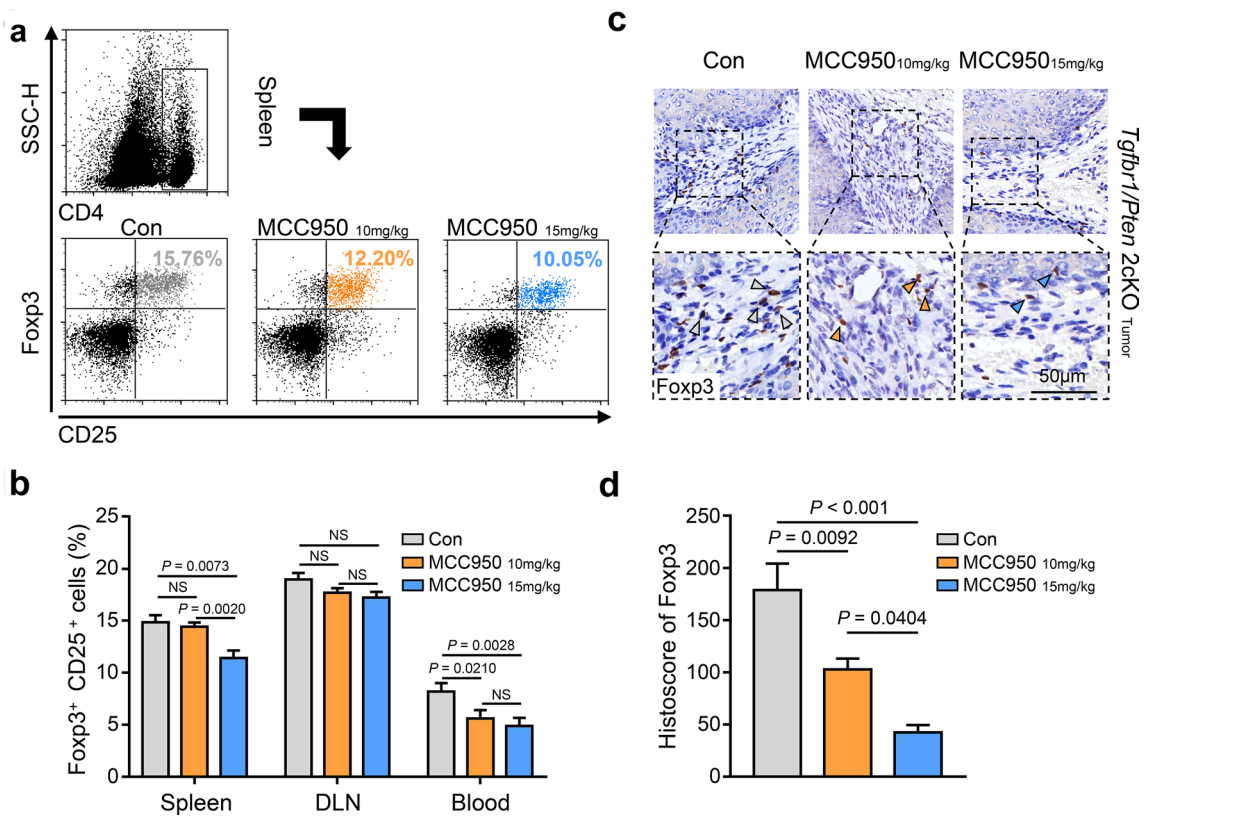

Fig. 3 Inhibition of NLRP3 inflammasome decreased the population of regular T cells in a HNSCC mouse model. **a** Flow cytometry shows the population variation of $CD4^+CD25^+Foxp3^+$ Tregs in the spleen of PBS- and MCC950-treated mice. **b** Quantification and statistical analysis of regular T cell ratio in $CD4^+$ cells among three groups (data shown as mean ± SEM). **c** Representative immunohistochemical staining images show the density difference of Foxp3-positive cells in *Tgfbr1*/*Pten*2cKO mice tumors of three groups; scale bar = 50 μm; the arrow points to positive staining. **d** Quantification of IHC histoscore of Foxp3 (data shown as mean ± SEM)

(Fig. 4a–c). In addition, immunofluorescence staining further confirmed that MCC950 treatment could reduce the population of $CD11b^+LY6G^+$ granulocytic MDSCs in the tumor microenvironment (Fig. 4e, f). CCL2 and CXCL1 are critical chemokines for the recruitment of MDSCs and TAMs [34, 35]. Western blot analysis supported the finding that CCL2 and CXCL1 expression was reduced, which was accompanied by a decrease in IL-1β in mouse tumor tissues (Fig. 4d). Similarly, we noticed a decreasing trend in TAMs after the inactivation of NLRP3, and this tendency of reduction was more evident in the 15 mg/kg MCC950 treatment group (Fig. 5a). However, this change was statistically significant only in the tumor tissue (Fig. 5b). Beyond that, because the CD47–SIRPα axis between tumor cells and immune cells is an important molecular pattern for tumor immune escape and blocking this signaling can enhance phagocytosis of tumor cells [36], we performed western blot and immunofluorescence to examine the expression level of CD47–SIRPα axis proteins. The results showed that MCC950 treatment significantly decreased the expression levels of CD47 and SIRPα in the tumor tissues of 2cKO tumor-bearing mice (Fig. 5c); the immunofluorescence results also confirmed this finding (Fig. 5d).

Blockade of the NLRP3 inflammasome increased the number of effective $CD4^+$ and $CD8^+$ T cells in a mouse model of HNSCC

Our previous studies verified that 2cKO tumor-bearing mice are in an immunosuppressive state, which is accompanied by a decreasing trend of $CD4^+$ and $CD8^+$ T cells and an increasing trend of PD-1- or Tim3-exhausted T cells compared with wild-type mice [20, 21]. Given these findings, flow cytometry was used to detect the proportional changes in those T cells after MCC950 treatment (Fig. 6a). We found that the populations of $CD4^+$ T cells in the DLN and $CD8^+$ T cells in the spleen were significantly elevated when the mice were treated with 10 mg/kg MCC950. $CD4^+$ and $CD8^+$ T cells were also significantly increased in number in the spleen, DLN, and blood when the mice were treated with 15 mg/kg MCC950 ($^*p < 0.05$; $^{**}p < 0.01$; $^{***}p < 0.001$; Fig. 6a, b). In contrast, the numbers of PD-1^+ $CD4^+$ T cells and $Tim3^+$ $CD4^+$ T cells

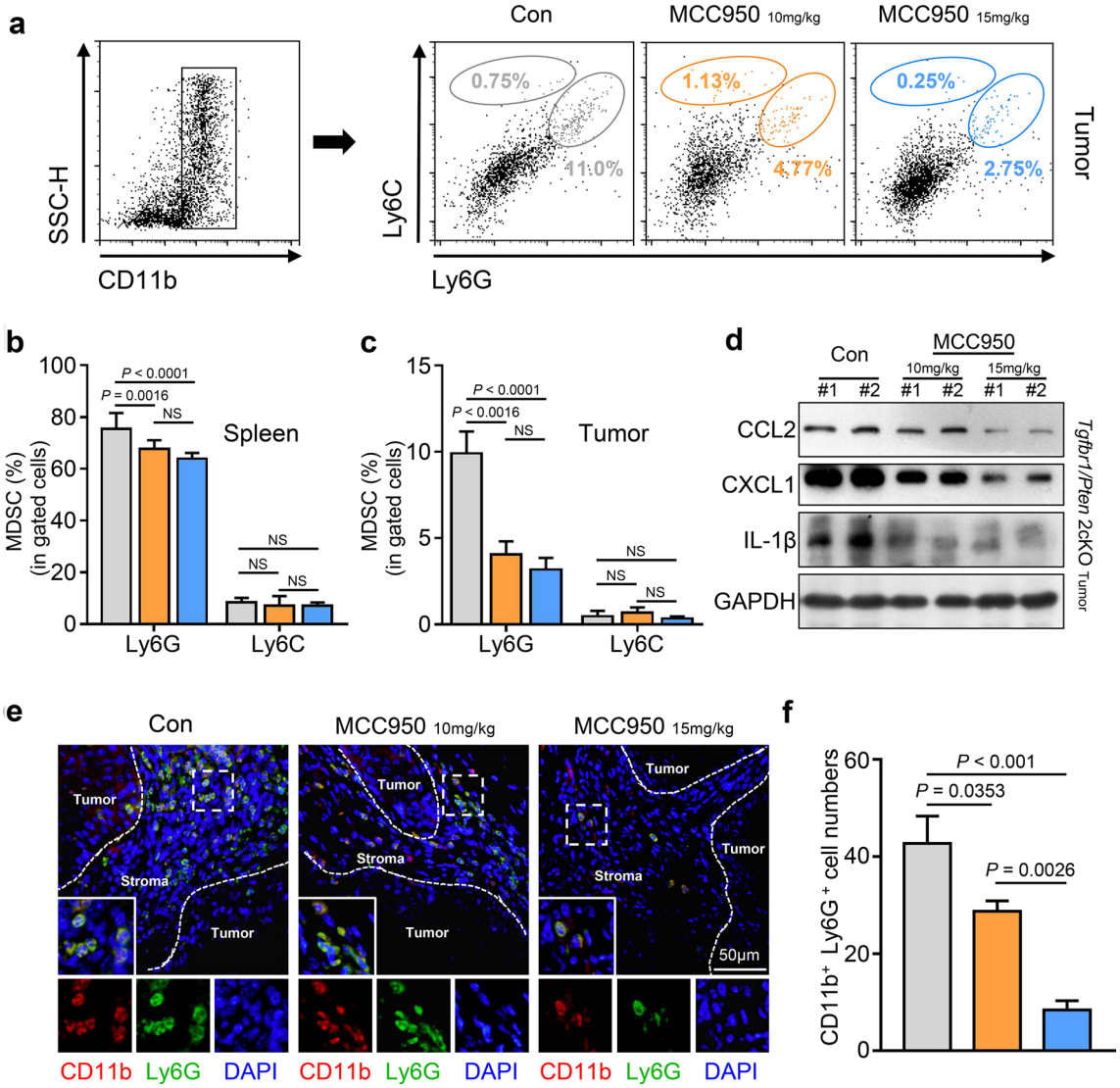

Fig. 4 Blockaded NLRP3 inflammasome activation by MCC950 could effectively reduce the recruitment of myeloid-derived suppressor cells in a *Tgfbr1*/*Pten* 2cKO HNSCC mouse model. **a** Flow cytometry dot plots for MDSCs isolated from control and MCC950-treated 2cKO tumor-bearing mice. **b**, **c** Quantification and statistical analysis show MCC950 treatment decreased the populations of MDSCs in HNSCC mice spleen and tumor (data shown as mean ± SEM). **d** The expression of IL-1β and MDSCs associated cytokines, CCL2 and CXCL1, in tumors were analyzed by western blot after HNSCC mice received PBS or anti-NLRP3 activation treatments. **e** Representative immunofluorescence microscopy images of granulocytic MDSCs ($CD11b^+Ly6G^+$) in the control or MCC950-treated mice tumor tissue. CD11b in red, Ly6G in green and DAPI in blue; scale bar = 50 μm. **f** Quantitative analysis of CD11b- and Ly6G-positive cells in three groups (data shown as mean ± SEM). In the histogram, Gray = control group, yellow = 10 mg/kg MCC950 group and blue = 15 mg/kg MCC950 group

in the spleen and DLN were reduced when the mice were treated with 10 mg/kg MCC950, and the numbers of $PD\text{-}1^+$ $CD8^+$ T cells in the spleen and blood and $Tim3^+$ $CD8^+$ T cells in the DLN and blood were also decreased in the 10 mg/kg MCC950 group. Moreover, a significant reduction in $PD\text{-}1^+$ and $Tim3^+$ T cell was observed in the spleen, DLN, and blood in mice that were treated with 15 mg/kg MCC950 (*$p < 0.05$; **$p < 0.01$; ***$p < 0.001$; Fig. 6c, d). Furthermore, immunochemistry showed that the numbers of $CD4^+$ and $CD8^+$ T cells were increased in tumor tissues after MCC950 treatment (Fig. 6e, f) and that the numbers of PD-1- and Tim3-positive cells were remarkably reduced after MCC950 treatment compared with the control group (Fig. 6e, f).

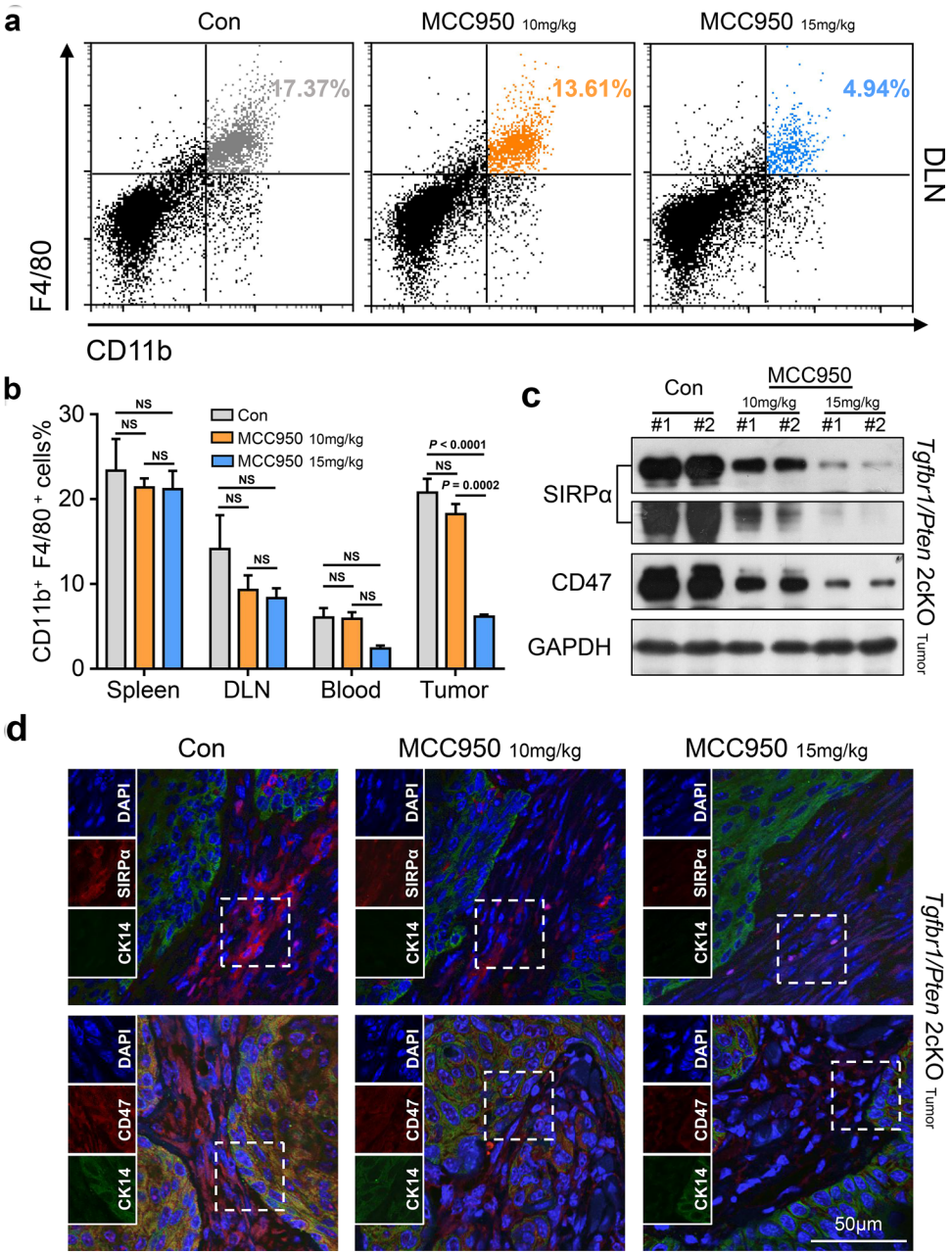

Fig. 5 TAMs were remarkably dropped by MCC950 treatment in the tumor microenvironment of a HNSCC mouse model. **a** Flow cytometry dot plots for $CD11b^{+}F4/80^{+}$ tumor-associated macrophages in the control group and MCC950 treated group in DLN. **b** Quantification and significant difference in TAM accumulations among four tissues of 2cKO tumor-bearing mice (data shown as mean ± SEM). **c** Western blot analysis shows that the expression level of SIRPα and CD47 was obviously dropped after MCC950 treatment in *Tgfbr1*/*Pten* 2cKO mice tumors. **d** Representative immunofluorescence microscopy images of SIRPα (red), CD47 (red), DAPI (blue) and CK-14 (green) in PBS or MCC950 treated mice tumor tissue; scale bar = 50 μm

The expression of NLRP3 inflammasome was positively correlated with CD4, CD8, Tregs, MDSCs, TAMs and the immune checkpoint proteins PD-1 and Tim3 in human HNSCC

To further investigate the clinical significance of the NLRP3 inflammasome in human HNSCC, the relationships among the NLRP3 inflammasome and Tregs, CD4, CD8, MDSCs, TAMs and the immune checkpoint proteins PD-1 and Tim3 were analyzed in a human HNSCC tissue array (12 oral mucosa samples, 38 dysplasia cases and 64 HNSCC cases). By immunohistochemical analysis, we found that the NLRP3 inflammasome was positively correlated with the following: CD4 expression ($p < 0.001$, $r = 0.3884$), CD8 expression ($p < 0.01$, $r = 0.2752$), the Treg marker Foxp3, $p < 0.001$, $r = 0.4081$), the MDSC markers CD11b and CD33 ($p < 0.001$, $r = 0.3925$; $p < 0.001$, $r = 0.3535$), the TAM markers CD68 and CD163 ($p = 0.001$, $r = 0.3514$; $p < 0.01$, $r = 0.2934$), PD-1 ($p < 0.05$, $r = 0.2053$) and Tim3 ($p < 0.001$, $r = 0.4209$) (Fig. 7a, b). Interestingly, the expression of the NLRP3 inflammasome components caspase-1, ASC and IL-18 was also closely related to the expression of those proteins (Fig. S2). Hierarchical clustering analyses provided us with an intuitive understanding of the correlation among those proteins (Fig. 7c). The data described above verified that the NLRP3 inflammasome

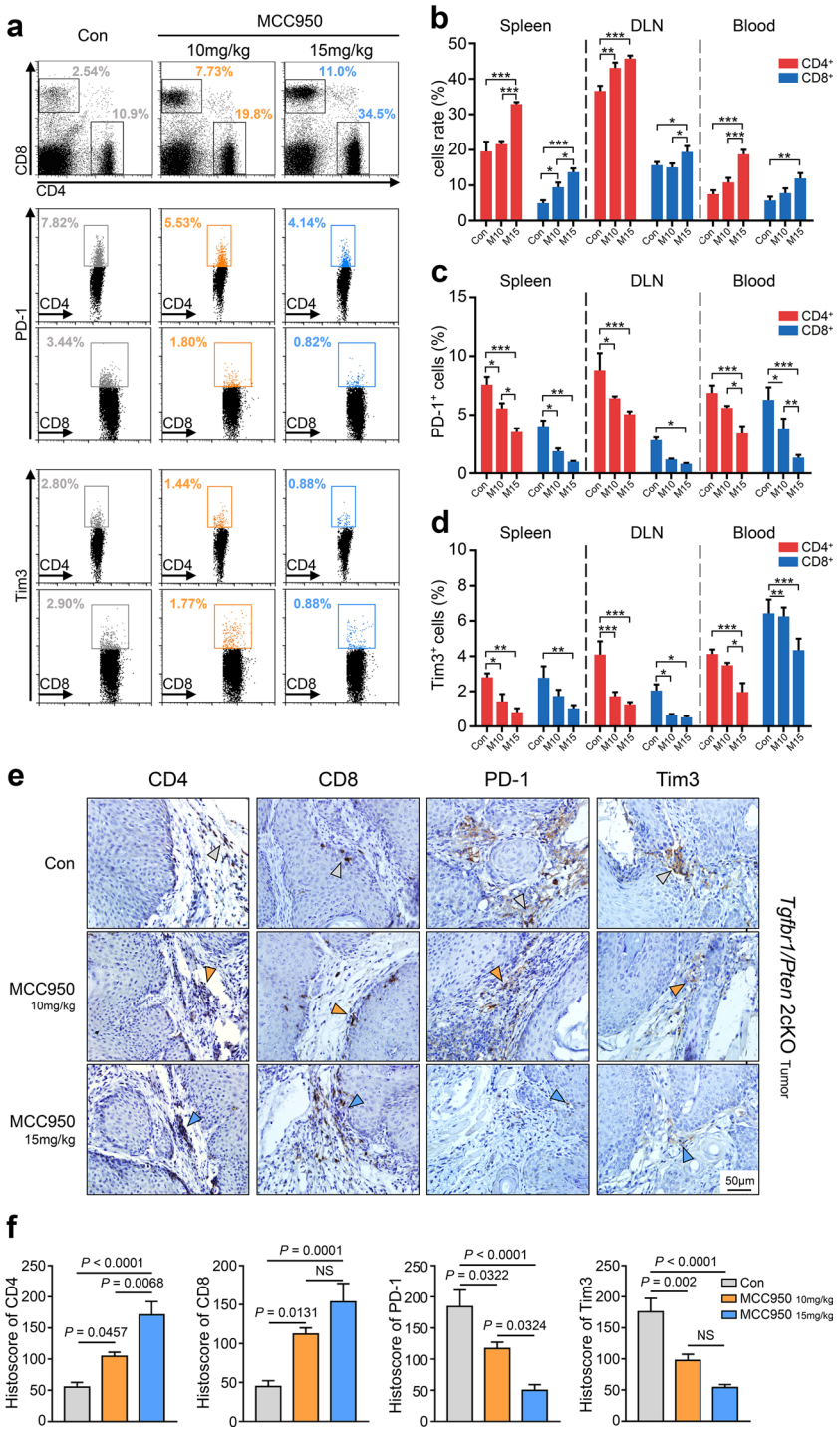

Fig. 6 NLRP3 inflammasome inactivation increased effector T cells and decreased exhausted T cells in *Tgfbr1*/*Pten* 2cKO mice. **a** Flow cytometry analysis of effector CD4$^+$ and CD8$^+$ T cells, PD-1$^+$ T cell and Tim3$^+$ T cell populations in spleens of PBS- or MCC950- treated mice. **b** Quantification and statistical analysis of CD4$^+$ (red) and CD8$^+$ (blue) T cells in spleen, DLN and blood (M10 = 10 mg/kg MCC950; M15 = 15 mg/kg MCC950, $*p < 0.05$; $**p < 0.01$; $***p < 0.001$). **c** Quantification and statistical analysis results of PD-1$^+$ T cell proportion in CD4$^+$ (red) and CD8$^+$ (blue) T cells in three groups ($*p < 0.05$; $**p < 0.01$; $***p < 0.001$). **d** Variation of Tim3$^+$ T cell ratio in CD4$^+$ (red) and CD8$^+$ (blue) T cells in three groups ($*p < 0.05$; $**p < 0.01$; $***p < 0.001$). **e**, **f** Representative immunohistochemical staining and quantification of CD4, CD8, PD-1, and Tim3 in *Tgfbr1*/*Pten* 2cKO mice tumor tissues after PBS or MCC950 treatments; scale bars = 50 μm, the arrow points to positive staining

was associated with effector CD4 and CD8 T cells, Tregs, MDSCs, TAMs and the immune checkpoint proteins PD-1 and Tim3.

The NLRP3 inflammasome proteins were up-regulated in both human HNSCC and *Tgfbr1*/*Pten* 2cKO HNSCC mice (Fig. 1). Apart from this finding, we found that the *IL-1B* mRNA level was closely related to NLRP3 expression in head and neck squamous cell carcinoma by querying the publicly available TCGA database (Fig. S1b, $p < 0.001$, $r = 0.3558$). However, considering that the use of MCC950 to block the activation of the NLRP3 inflammasome only reduced the secretion of inflammatory factors [37], consequently, the most direct effect was observed when mice were treated with MCC950, which reduced the secretion of IL-1β. This effect was accompanied by an improvement in the inflammatory environment, which

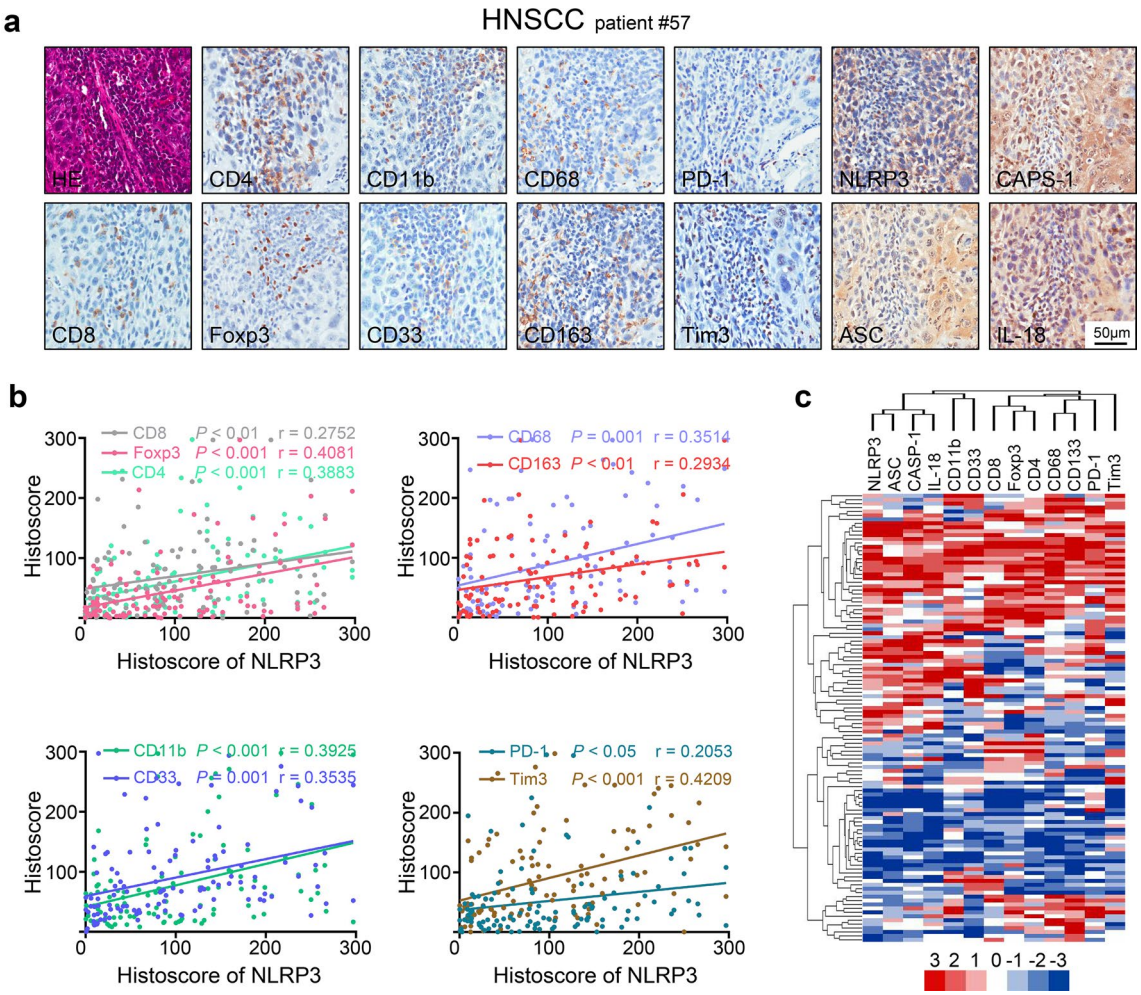

Fig. 7 NLRP3 inflammasome expression pattern displays a correlation with CD4, CD8, PD-1, Tim3 and Treg, MDSC and TAM associated proteins in human HNSCC. **a** Serial section with immunohistochemical staining of NLRP3 inflammasome components and CD4, CD8, Fopx3, CD11b, CD33, CD68, CD163, PD-1, and Tim3 in human HNSCC tissue (tissue microarray, patient number 57); scale bars = 50 μm. **b** Expression of NLRP3 was significant and positively associated with CD4 ($p < 0.001$, $r = 0.3883$), CD8 ($p < 0.01$, $r = 0.2752$), Foxp3 ($p < 0.001$, $r = 0.4081$), CD11b($p < 0.001$, $r = 0.3925$), CD33 ($p < 0.001$, $r = 0.3535$), CD68 ($p < 0.001$, $r = 0.3514$), CD163 ($p < 0.01$, $r = 0.2934$), PD-1 ($p < 0.05$, $r = 0.2053$) and Tim3 ($p < 0.001$, $r = 0.4209$) by Spearman's rank correlation coefficient test and linear tendency test. **c** Hierarchical clustering plot of the expression patterns of these markers in HNSCC tissue microarray, which contains 64 HNSCC, 12 dysplasia, 38 mucosae

slowed tumor progression. As a result, we speculated that the enhancement of antitumor immunity by MCC950 treatment in this HNSCC mouse model (*Tgfbr1*/*Pten* 2cKO) was achieved by the inhibition of NLRP3 inflammasome.

Discussion

Currently, chronic inflammation is thought to function as a tumor promoter that leads to an immunosuppressive state [18], and a variety of cytokines or chemokines stimulate the production and recruitment of immunosuppressive cells [18, 38]. HNSCC is an immunosuppressive and inflammation-related tumor type [11, 39], and the NLRP3 inflammasome is considered the widest harmful stimuli sensor of innate immunity [40]. However, until now, the relationship between the inflammatory microenvironment and tumor immunity was not fully understood. Our previous study demonstrated that NLRP3 inflammasome promotes tumorigenesis in HNSCC [41]. In this study, we uncovered that activation of the NLRP3 inflammasome/IL-1β pathway in human and murine HNSCC provided an inflammatory microenvironment that promoted HNSCC progression. The results show that activation of the NLRP3 inflammasome, which was inhibited by MCC950, led to a reduction in the secretion of IL-1β and an accompanied delay in tumorigenesis in spontaneous de novo *Tgfbr1*/*Pten* 2cKO HNSCC mice. Inhibition of the NLRP3 inflammasome also diminished the infiltration

of immunosuppressive cells, such as Tregs, MDSCs and TAMs, and enhanced T cell function via an increase in TILs and a reduction in PD-1- and Tim3-exhausted T cells. Moreover, the expression of the NLRP3 inflammasome was correlated with the expression of CD4, CD8, Foxp3, CD11b, CD33, CD68, CD163, PD-1 and Tim3 according to a human HNSCC tissue array.

The NLRP3 inflammasome is considered to be a double-edged sword in the cancer immunity [4] and it can help the body remove harmful pathogens but can also be activated in a variety of tumors and promote tumor development. On the one hand, the effect of the NLRP3 inflammasome has tissue specificity [42, 43]; thus, interpretation of the roles of the inflammasome in cancer development has to consider tissue type. On the other hand, due to the complexity of the components of the NLRP3 inflammasome, the role of each component in the tumor is not the same: IL-1β was reported to promote tumor growth, but the absence of IL-18, ASC, and caspase-1 increases the probability of a tumor in mice with gastric cancer [43–45]. In addition, the NLRP3 inflammasome is an important component of innate immunity and can hence sense various signals, including those not associated with cancer cells [5]. Therefore, the NLRP3 inflammasome indeed provides a promising target for cancer therapy, but more studies are needed to identify the specific molecular mechanisms of the NLRP3 inflammasome during cancer development and progression. IL-1β and IL-18 are the main downstream products of the NLRP3 inflammasome; nevertheless, the role of IL-18 in tumorigenesis is controversial. The activation of IL-18 may promote tumor development or, conversely, enhance antitumor immunity and limit tumor growth by the activation of NK and T cell responses [46]. It has also been reported that tumor growth was not reduced in IL-18 KO mice but can be reduced with the decrease in IL-1β [16], and there is abundant evidence that shows that IL-1β is a tumor-promoting cytokine [16, 47]. Given these factors, our work focused on IL-1β. The inflammasome is not only expressed in stromal cells but also in cancer cells, so that these "new sensors" within the tumor site will produce large amounts of abnormal IL-1β through the activation of the NLRP3 inflammasome. In this report, IL-1β was found to be overexpressed in the serum of HNSCC patients and in multiple tissues in a mouse model of HNSCC, which suggests that IL-1β may be a crucial component in promoting tumor growth in HNSCC. Subsequent studies were based on a selective small molecule inhibitor of the NLRP3 inflammasome, MCC950, which inhibits the NLRP3 inflammasome via the inhibition of ASC oligomerization rather than via the reduction in NLRP3 inflammasome protein expression to decrease the production of IL-1β [37]. Our study indicated that the reduction of IL-1β can effectively slow down the tumor burdened speed in HNSCC mice.

The multiple tumorigenic mechanisms that occur in the *Tgfbr1*/*Pten* 2cKO HNSCC mouse model make it suitable for the study of human HNSCC [24]. Similar to human HNSCC, the immune system of 2cKO tumor-bearing mice is also in an inhibited state and characterized by an accumulation of MDSC, Treg and TAM subsets [21]. Studies have found that IL-1β can increase the number of MDSCs [47], which damages immune function in mammary and gastric carcinomas [37], affects the number of TAMs in a mouse model of lung cancer [48] and is related to the increase in Tregs in melanoma [49]. Guo et al. found that the NLRP3 inflammasome/IL-1β pathway promoted tumor growth and metastasis and may account for the recruitment of MDSCs and TAMs in the tumor environment in breast cancer [16]. Nevertheless, the relationship between elevated IL-1β and the presence of immunosuppressive cells in HNSCC is not clear. In this study, the inhibition of NLRP3 inflammasome resulted in a sharp decline in the concentration of IL-1β and reduced the number of immunosuppressive cells in an HNSCC mouse model. The number of $CD4^+Foxp3^+CD25^+$ regular T cells in the blood, spleen and tumor samples were remarkably decreased. Interestingly, we found that the number of $CD11b^+LY6G^+LY6C^{low}$ granulocytic MDSCs, rather than $CD11b^+LY6G^-LY6C^{high}$ monocytic MDSCs, was obviously changed, which was consistent with a current report that $LY6C^{low}$ granulocytic MDSCs were predominant in tumors and that they impaired NK cells in vitro and in vivo [50]. TAMs play an important role in the development of neoplasia, and its infiltration is correlated with poor prognosis of HNSCC patients [51]. TAMs are one of the main producers of IL-1β, and the inflammatory environment can also promote the recruitment of TAMs [47]. Recent research indicated that tumor-associated macrophages promote metastasis via the NLRP3/IL-1β pathway [52]. Additionally, the chemokines CCL2 and CXCL1 are important for the recruitment of MDSCs and TAMs [34, 53], and the reduction of CCL2 and CXCL1 in MCC950-treated mice also supports our results. The CD47/SIPα axis acts as a "do not eat me" signal in malignant tumors, which may facilitate tumor immune escape, and the inhibition of this pathway can enhance the phagocytosis of cancer cells by macrophages [36]. The results show that MCC950 treatment may have different effects on different peripheral immune organs and circulation; however, the underlying mechanism is still unclear.

Recently, emerging immunotherapies based on immune checkpoints have shown promising prospects for future cancer treatment. Programmed death-1 (PD-1) and T cell immunoglobulin mucin-3 (Tim3) are expressed on TILs, and it is commonly recognized that the expression of PD-1 or/and Tim3 impairs T cell function [54]; when PD-1/Tim3-positive T cells are recognized among tumor cells, tumor escape may occur [54]. In the present study, we found that the populations of $CD4^+$ and $CD8^+$ T cells were significantly increased

and that the amount of PD-1- and Tim3-positive T cells were significantly diminished when the NLRP3 inflammasome/IL-1β pathway was inhibited. Our results indicated that after MCC950 treatment, the number of exhausted T cells and the damage to T cells decreased.

In summary, we demonstrated that NLRP3 inflammasome/IL-1β signaling induces the inflammatory microenvironment to promote tumorigenesis and the development of HNSCC. NLRP3 inflammasome inhibition delayed tumor growth and reshaped the antitumor response through a decrease in the number of immunosuppressive cells and an enhancement in the function of effector T cells in the *Tgfbr1*/*Pten* 2cKO HNSCC mouse model. These data suggest that the inhibition of the tumor microenvironment through the NLRP3 inflammasome/IL-1β pathway may provide a novel approach for HNSCC therapy.

Acknowledgements This work was supported by National Natural Science Foundation of China 81402241, 81672667, 81672668, 81472528, 81472529.

Compliance with ethical standards

Ethical standards Animal studies were approved and supervised by the Animal Care and Use Committee of Wuhan University. All human studies obtained informed consent from patients at the beginning of the trial and were approved by the Medical Ethics Committee of the Hospital of Stomatology, Wuhan University. The ethical approval number is 2014C66.

Conflict of interest The authors declare that they have no conflict of interest.

References

1. Grivennikov SI, Greten FR, Karin M (2010) Immunity, inflammation, and cancer. Cell 140(6):883–899
2. Coussens LM, Zitvogel L, Palucka AK (2013) Neutralizing tumor-promoting chronic inflammation: a magic bullet? Science 339(6117):286–291
3. Próchnicki T, Mangan MS, Latz E (2016) Recent insights into the molecular mechanisms of the NLRP3 inflammasome activation. F1000Res 5:1469
4. Kolb R, Liu GH, Janowski AM, Sutterwala FS, Zhang W (2014) Inflammasomes in cancer: a double-edged sword. Protein Cell 5(1):12–20
5. Menu P, Vince JE (2011) The NLRP3 inflammasome in health and disease: the good, the bad and the ugly. Clin Exp Immunol 166(1):1
6. Li Y, Wang L, Pappan L, Galliher-beckley A, Shi J (2012) IL-1β promotes stemness and invasiveness of colon cancer cells through Zeb1 activation. Mol Cancer 11(1):87
7. Abrahamsson A, Morad V, Saarinen NM, Dabrosin C (2012) Estradiol, tamoxifen, and flaxseed alter IL-1β and IL-1Ra levels in normal human breast tissue in vivo. J Clin Endocrinol Metab 97(11):2044–2054
8. Chen W, Zheng R, Baade PD, Zhang S, Zeng H, Bray F, Jemal A, Yu XQ, He J (2016) Cancer statistics in China. CA Cancer J Clin 66(2):115–132
9. Hunter KD, Parkinson EK, Harrison PR (2005) Profiling early head and neck cancer. Nat Rev Cancer 5(2):127–135
10. Warnakulasuriya S (2009) Global epidemiology of oral and oropharyngeal cancer. Oral Oncol 45(4–5):309
11. Ferris RL (2015) Immunology and immunotherapy of head and neck cancer. J Clin Oncol 33(29):3293
12. Ferris RL, Whiteside TL, Ferrone S (2006) Immune escape associated with functional defects in antigen-processing machinery in head and neck cancer. Clin Cancer Res 12(13):3890–3895
13. Dasgupta S, Bhattacharyachatterjee M, O'Malley BW Jr, Chatterjee SK (2005) Inhibition of NK cell activity through TGF-beta 1 by down-regulation of NKG2D in a murine model of head and neck cancer. J Immunol 175(8):5541–5550
14. Kuss I, Hathaway B, Ferris RL, Gooding W, Whiteside TL (2004) Decreased absolute counts of T lymphocyte subsets and their relation to disease in squamous cell carcinoma of the head and neck. Clin Cancer Res 10(11):3755–3762
15. Economopoulou P, Kotsantis I, Psyrri A (2016) Checkpoint inhibitors in head and neck cancer: rationale, clinical activity, and potential biomarkers. Curr Treat Options Oncol 17(8):40
16. Guo B, Fu S, Zhang J, Liu B, Li Z (2016) Targeting inflammasome/IL-1 pathways for cancer immunotherapy. Sci Rep 6:36107
17. Gajewski TF, Woo SR, Zha Y, Spaapen R, Zheng Y, Corrales L, Spranger S (2013) Cancer immunotherapy strategies based on overcoming barriers within the tumor microenvironment. Curr Opin Immunol 25(2):268–276
18. Kanterman J, Sadefeldman M, Baniyash M (2012) New insights into chronic inflammation-induced immunosuppression. Semin Cancer Biol 22(4):307–318
19. Bruchard M, Mignot G, Derangère V, Chalmin F, Chevriaux A, Végran F, Boireau W, Simon B, Ryffel B, Connat JL (2013) Chemotherapy-triggered cathepsin B release in myeloid-derived suppressor cells activates the Nlrp3 inflammasome and promotes tumor growth. Nat Med 19(1):57–64
20. Yu GT, Bu LL, Zhao YY, Mao L, Deng WW, Wu TF, Zhang WF, Sun ZJ (2016) CTLA4 blockade reduces immature myeloid cells in head and neck squamous cell carcinoma. Oncoimmunology 5(6):e1151594
21. Deng WW, Mao L, Yu GT, Bu LL, Ma SR, Liu B, Gutkind JS, Kulkarni AB, Zhang WF, Sun ZJ (2016) LAG-3 confers poor prognosis and its blockade reshapes antitumor response in head and neck squamous cell carcinoma. Oncoimmunology 5(11):e1239005
22. Moynihan KD, Opel CF, Szeto GL, Tzeng A, Zhu EF, Engreitz JM, Williams RT, Rakhra K, Zhang MH, Rothschilds AM, Kumari S, Kelly RL, Kwan BH, Abraham W, Hu K, Mehta NK, Kauke MJ, Suh H, Cochran JR, Lauffenburger DA, Wittrup KD, Irvine DJ (2016) Eradication of large established tumors in mice by combination immunotherapy that engages innate and adaptive immune responses. Nat Med 22(12):1402–1410
23. Yu GT, Bu LL, Huang CF, Zhang WF, Chen WJ, Gutkind JS, Kulkarni AB, Sun ZJ (2015) PD-1 blockade attenuates immunosuppressive myeloid cells due to inhibition of CD47/SIRPα axis in HPV negative head and neck squamous cell carcinoma. Oncotarget 6(39):42067–42080
24. Bian Y, Hall B, Sun ZJ, Molinolo A, Chen W, Gutkind JS, Waes CV, Kulkarni AB (2012) Loss of TGF-β signaling and PTEN promotes head and neck squamous cell carcinoma through cellular senescence evasion and cancer-related inflammation. Oncogene 31(28):3322–3332
25. Eisen MB, Spellman PT, Brown PO, Botstein D (1998) Cluster analysis and display of genome-wide expression patterns. Proc Natl Acad Sci USA 95(25):14863–14868

26. Saldanha AJ (2004) Java Treeview—extensible visualization of microarray data. Bioinformatics 20(17):3246–3248
27. Peng CH, Liao CT, Peng SC, Chen YJ, Cheng AJ, Juang JL, Tsai CY, Chen TC, Chuang YJ, Tang CY, Hsieh WP, Yen TC (2011) A novel molecular signature identified by systems genetics approach predicts prognosis in oral squamous cell carcinoma. PLoS One 6(8):e23452
28. Ye H, Yu T, Temam S, Ziober BL, Wang J, Schwartz JL, Mao L, Wong DT, Zhou X (2008) Transcriptomic dissection of tongue squamous cell carcinoma. BMC Genom 9(1):69
29. Ginos MA, Page GP, Michalowicz BS, Patel KJ, Volker SE, Pambuccian SE, Ondrey FG, Adams GL, Gaffney PM (2004) Identification of a gene expression signature associated with recurrent disease in squamous cell carcinoma of the head and neck. Cancer Res 64(1):55
30. Putz G, Rosner AI, Schmitz N, Buchholz F (2006) AML1 deletion in adult mice causes splenomegaly and lymphomas. Oncogene 25(6):929–939
31. Xie P, Stunz LL, Larison KD, Yang B, Bishop GA (2007) TRAF3 is a critical regulator of B cell homeostasis in secondary lymphoid organs. Immunity 27(2):253–267
32. Zou W (2006) Regulatory T cells, tumour immunity and immunotherapy. Nat Rev Immunol 6(4):295
33. Je-In Youn SN, Collazo Michelle, Gabrilovich Dmitry I (2008) Subsets of myeloid-derived suppressor cells in tumor-bearing mice. J Immunol 181(8):5791–5802
34. Chang AL, Miska J, Wainwright DA, Dey M, Rivetta CV, Yu D, Kanojia D, Pituch KC, Qiao J, Pytel P (2016) CCL2 produced by the glioma microenvironment is essential for the recruitment of regulatory T cells and myeloid-derived suppressor cells. Cancer Res 76(19):5671
35. Sander LE, Sackett SD, Dierssen U, Beraza N, Linke RP, Müller M, Blander JM, Tacke F, Trautwein C (2010) Hepatic acute-phase proteins control innate immune responses during infection by promoting myeloid-derived suppressor cell function. J Exp Med 207(7):1453–1464
36. Mccracken MN, Cha AC, Weissman IL (2015) Molecular pathways: activating T cells after cancer cell phagocytosis from blockade of CD47 "don't eat me" signals. Clin Cancer Res 21(16):3597–3601
37. Shao BZ, Xu ZQ, Han BZ, Su DF, Liu C (2015) NLRP3 inflammasome and its inhibitors: a review. Front Pharmacol 6:262
38. Solito S, Marigo I, Pinton L, Damuzzo V, Mandruzzato S, Bronte V (2014) Myeloid-derived suppressor cell heterogeneity in human cancers. Ann N Y Acad Sci 1319(1):47–65
39. Yang X, Lu H, Yan B, Romano RA, Bian Y, Friedman J, Duggal P, Allen C, Chuang R, Ehsanian R (2011) ΔNp63 versatilely regulates a Broad NF-κB gene program and promotes squamous epithelial proliferation, migration, and inflammation. Cancer Res 71(10):3688–3700
40. Guo H, Callaway JB, Ting JP (2015) Inflammasomes: mechanism of action, role in disease, and therapeutics. Nat Med 21(7):677
41. Huang CF, Chen L, Li YC, Wu L, Yu GT, Zhang WF, Sun ZJ (2017) NLRP3 inflammasome activation promotes inflammation-induced carcinogenesis in head and neck squamous cell carcinoma. J Exp Clin Cancer Res 36(1):116
42. Okamoto M, Liu W, Luo Y, Tanaka A, Cai X, Norris DA, Dinarello CA, Fujita M (2010) Constitutively active inflammasome in human melanoma cells mediating autoinflammation via caspase-1 processing and secretion of interleukin-1beta. J Biol Chem 285(9):6477–6488
43. Allen IC, TeKippe EM, Woodford RM, Uronis JM, Holl EK, Rogers AB, Herfarth HH, Jobin C, Ting JP (2010) The NLRP3 inflammasome functions as a negative regulator of tumorigenesis during colitis-associated cancer. J Exp Med 207(5):1045–1056
44. Zaki MH, Vogel P, Bodymalapel M, Lamkanfi M, Kanneganti TD (2010) IL-18 production downstream of the Nlrp3 inflammasome confers protection against colorectal tumor formation. J Immunol 185(8):4912
45. Dupaul-Chicoine J, Yeretssian G, Doiron K, Bergstrom KSB, Meunier C, Gros P, Vallance BA, Saleh M, Mcintire CR, Leblanc PM (2010) Control of intestinal homeostasis, colitis, and colitis-associated colorectal cancer by the inflammatory caspases. Immunity 32(3):367
46. Fabbi M, Carbotti G, Ferrini S (2015) Context-dependent role of IL-18 in cancer biology and counter-regulation by IL-18BP. J Leukoc Biol 97(4):665
47. Tu S, Bhagat G, Cui G, Takaishi S, Kurt-Jones EA, Rickman B, Betz KS, Penz-Oesterreicher M, Bjorkdahl O, Fox JG, Wang TC (2011) Overexpression of interleukin-1beta induces gastric inflammation and cancer and mobilizes myeloid-derived suppressor cells in mice. Cancer Cell 14(5):408–419
48. Terlizzi M, Colarusso C, Popolo A, Pinto A, Sorrentino R (2016) IL-1α and IL-1β-producing macrophages populate lung tumor lesions in mice. Oncotarget 7(36):58181–58182
49. Jiang H, Gebhardt C, Umansky L, Beckhove P, Schulze TJ, Utikal J, Umansky V (2015) Elevated chronic inflammatory factors and myeloid-derived suppressor cells indicate poor prognosis in advanced melanoma patients. Int J Cancer 136(10):2352–2360
50. Elkabets M, Ribeiro VS, Dinarello CA, Ostrand-Rosenberg S, Di SJ, Apte RN, Vosshenrich CA (2010) IL-1β regulates a novel myeloid-derived suppressor cell subset that impairs NK cell development and function. Eur J Immunol 40(12):3347–3357
51. Balermpas P, Rödel F, Liberz R, Oppermann J, Wagenblast J, Ghanaati S, Harter PN, Mittelbronn M, Weiss C, Rödel C (2014) Head and neck cancer relapse after chemoradiotherapy correlates with $CD163^+$ macrophages in primary tumour and $CD11b^+$ myeloid cells in recurrences. Br J Cancer 111(8):1509
52. Weichand B, Popp R, Dziumbla S, Mora J, Strack E, Elwakeel E, Frank A, Scholich K, Pierre S, Syed S (2017) S1PR1 on tumor-associated macrophages promotes lymphangiogenesis and metastasis via NLRP3/IL-1β. J Exp Med 214(9):2695–2713
53. Zarif JC, Taichman RS, Pienta KJ (2014) TAM macrophages promote growth and metastasis within the cancer ecosystem. Oncoimmunology 3(7):e941734
54. Pardoll DM (2012) The blockade of immune checkpoints in cancer immunotherapy. Nat Rev Cancer 12(4):252–264